Available online at www.sciencedirect.com

ScienceDirect

journal homepage: www.elsevier.com/locate/he

Ammonia decomposition over Ru-coated metal-structured catalysts for COx-free hydrogen production

Kee Young Koo [a,b,*], *Hyo Been Im* [a], *Dahye Song* [a], *Unho Jung* [a,**]

[a] *Hydrogen Research Department, Korea Institute of Energy Research (KIER), 152 Gajeong-ro, Yuseong-gu, Daejeon 34129, Republic of Korea*

[b] *Advanced Energy and System Engineering, University of Science and Technology (UST), 217 Gajeong-ro, Yuseong-gu, Daejeon, 34113, Republic of Korea*

HIGHLIGHTS

- COx-free H_2 production via NH_3 decomposition on Ru-coated metal-structured catalysts.
- Nano-sized Ru uniformly dispersed in plate-like Mg–Al oxide layers by precipitation.
- Amount of Ru in the structured catalyst was <~1/10 of that in the pellet catalyst.
- Foams performed better catalytically than monoliths at higher GHSV (6,000 h^{-1}).
- Foam catalyst stability was verified in a 20 Nm^3/h-H_2 production system for 100 h.

GRAPHICAL ABSTRACT

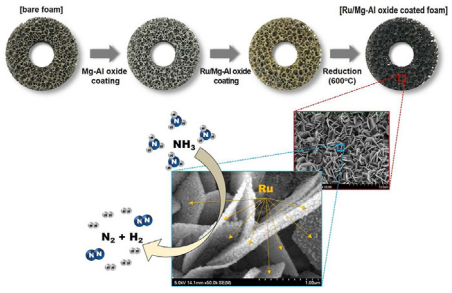

ARTICLE INFO

Article history:
Received 23 January 2023
Received in revised form
23 June 2023
Accepted 1 August 2023
Available online 17 August 2023

Keywords:
Ammonia decomposition
COx-free hydrogen
Ru catalyst

ABSTRACT

We report the development of Ru/Mg–Al oxide coated metal-structured catalysts with excellent heat and mass transfer characteristics for efficient clean H_2 production from ammonia decomposition. Ammonia is a promising carrier for the mass transport of hydrogen and facilitates the production of COx-free hydrogen by decomposing into nitrogen and hydrogen. Ru nanoparticles are uniformly dispersed on the Mg–Al oxide layer of the FeCralloy monoliths and foams via precipitation. The catalytic activities depend on the surface area and loading of the catalysts and the metal dispersion in the oxide layer. At temperatures <650 °C, and a gas hourly space velocity (GHSV) of 3,000 h^{-1}, monolithic catalysts with a large surface area and evenly distributed active metals perform excellently. Foam catalysts with excellent heat transfer performance better at temperatures

* Corresponding author.
** *Corresponding author.*
E-mail addresses: kykoo@kier.re.kr (K.Y. Koo), uhjung@kier.re.kr (U. Jung).

https://doi.org/10.1016/j.ijhydene.2023.08.004

Mg–Al oxide
Metal structured catalyst

>650 °C and GHSV >6,000 h^{-1}. Foam catalyst stability is verified for 100 h in a 20 Nm^3/h high-purity hydrogen production system.

1. Introduction

Decarbonizing energy systems have attracted worldwide attention, accelerating the research and applications of renewable energy, hydrogen energy, and carbon capture, utilization, and storage (CCUS) technologies to achieve carbon neutrality [1]. In particular, hydrogen energy plays a crucial role in replacing fossil fuels in various industries and power generation systems, and the demand for hydrogen energy is expected to increase [2]. However, the quality and quantity of renewable energy sources, such as solar and wind energies, depend on geographic locations. Australia, Chile, and the Middle Eastern countries have a competitive advantage in producing green hydrogen because of their abundant renewable energy resources. Hydrogen exportation from these countries is expected to be a driving force for new energy trade.

Hydrogen has a high energy density per unit mass (120 MJ/kg); however, on a volume basis, hydrogen energy density is very low, which notably increases the costs of long-distance transportation [4]. Thus, developing technologies to convert hydrogen into various types of carriers (ammonia, methanol, liquefied H_2, and methyl cyclohexane) is essential to overcome this limitation. Liquefied hydrogen requires expensive storage tanks at cryogenic temperatures (−253 °C) and qualified hydrogen supply infrastructure [3,4]. Comparatively, ammonia (NH_3) has a higher storage density per unit volume (121 kg-H_2/m^3) than that of liquid hydrogen (70.8 kg-H_2/m^3) and can be liquefied at room temperature (20 °C) and 8 atm pressure. Ammonia is more stable than hydrogen because of its low explosive limit and high flammability, and can be immediately detected in case of leakage. In terms of transportation and distribution, regular stainless-steel pipes and containers can be used to transport ammonia, and distribution networks are well-established internationally. Thus, ammonia is one of the most suitable hydrogen carriers as it enables economical transportation and eco-friendly hydrogen production [5,6].

The transported ammonia can be used directly for gas turbines, fuel cells (solid oxide fuel cells), and ammonia-capable industrial furnaces. Ammonia can also produce high-purity hydrogen via a clean process without emitting carbon dioxide [7]. In general, producing hydrogen from ammonia involves thermal decomposition ($2NH_3 \leftrightarrow N_2 + 3H_2$, $\Delta H^o = 92$ kJ/mol) followed by purification to remove small quantities of residual ammonia and nitrogen [4,8]. The required purity of the produced hydrogen depends on the final application. For instance, high-purity hydrogen (≥99.97%) with a residual NH_3 concentration below 0.1 ppm and N_2 concentration below 300 ppm is required for fuel cell vehicles according to ISO 14687 standard [9,10].

The traditional blue hydrogen production method is based on a natural gas (NG) reforming process, and multiple steps are involved, such as the pretreatment of raw materials (NG and H_2O), CH_4-steam reforming ($CH_4 + H_2O \leftrightarrow CO + 3H_2$, $\Delta H^o = 206.3$ kJ/mol) and water gas shift(WGS, $CO(g) + H_2O(g) \leftrightarrow CO_2(g) + H_2(g)$, $\Delta H^o = -41.1$ kJ/mol) reactions, pressure swing adsorption(PSA) for separation purification, and carbon capture and storage(CCS) (Fig. 1) [11]. By contrast, ammonia-based hydrogen production is a simple two-step process (decomposition and purification) with a single raw material (ammonia) [12]. Moreover, the low operating temperature of ammonia decomposition favors the maintenance of the catalyst activity. Compared with the NG reforming process, ammonia-based hydrogen production does not involve carbon deposition. Thus, the life of the catalyst and the efficiency of hydrogen production are both expected to increase. Ultimately, the advantages of ammonia decomposition compared with those of NG reforming should ensure that the former will be more economical.

However, the successful commercialization of ammonia decomposition technology has yet to be reported worldwide [6]. Major licensing companies for large-scale hydrogen production or ammonia synthesis (e.g., Haldor-topsoe, thyssenkrupp-Uhde, and KBR) are promoting the commercialization of ammonia decomposition hydrogen production processes by utilizing existing natural gas reforming processes and reforming catalysts.

Active catalysts with high durability and improved low-temperature activity have been synthesized to develop ammonia decomposition catalysts. Metals including Ru, Ni, Co, and Fe, have been studied as prospective active metals, and Ru-based catalysts demonstrated the best performances [4,13]. In general, Ru-based catalysts display good catalytic activity at low temperatures of ≤500 °C in the ammonia decomposition reaction. Li et al. [14] reported that the ammonia conversion accomplished by a Ru catalyst was higher than 20% of that by a Ni catalyst under the same reaction conditions and support. Furthermore, the support, which provides a large surface area, high metal dispersion, and displays high sinter-stability, has a marked effect on the catalytic activity in ammonia decomposition. In particular, the basicity of the support improves the recombinative desorption of surface nitrogen atoms (the rate-determining step) due to the electron donating properties [4]. Mg–Al oxide ($MgAlO_x$) has received much attention because it has a large surface area and displays good thermal stability at high temperatures while simultaneously imparting basicity [15]. A MgAlOx support can be prepared by a thermal treatment of

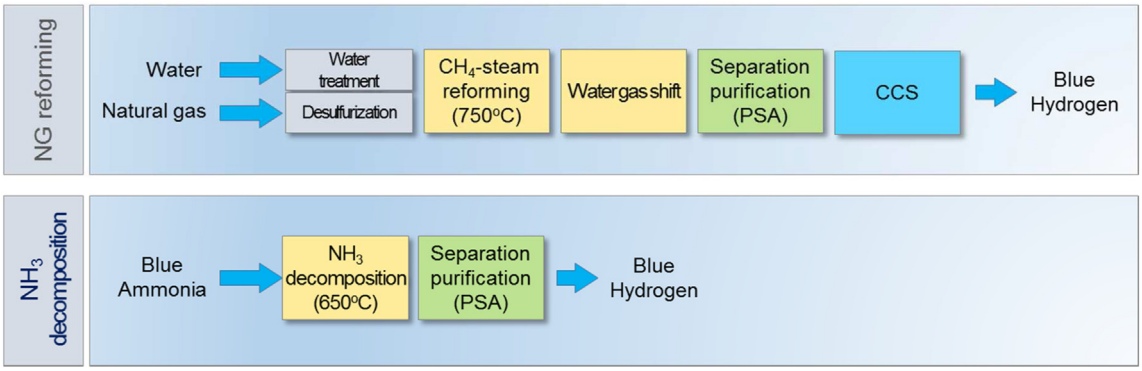

Fig. 1 – Comparison of process unit between natural gas (NG) reforming and NH_3 decomposition for the high-purity blue hydrogen production

Mg–Al layered double hydroxide (LDH). Moreover, Ru/$MgAlO_x$ catalysts have been used in various reactions, including NO storage/decomposition/reduction, glycerol steam reforming and carbon dioxide reforming of methane for the production of hydrogen and syngas, and ammonia synthesis [16–19]. Despite these advantages, few studies have been performed on a $MgAlO_x$ supported Ru catalyst system for ammonia decomposition [20,21].

In this study, Ru/Mg–Al oxide-coated metal-structured catalysts were unprecedentedly used to produce CO_x-free hydrogen via ammonia decomposition. Ammonia decomposition is endothermic, and effective external heat transfer is vital to improve hydrogen production efficiency. The metal-structured catalysts have a large ratio of the geometric reaction surface area to the reaction volume (S/V) and higher heat transfer rate per unit volume of process flow (US/V) [22]. Owing to the excellent heat and mass transfer, the catalysts in the forms of monoliths and foams can replace ceramic pellet catalysts in typical chemical processes and enable a compact reactor design [12,23]. However, the catalyst coating layer detaches easily from the metal substrate because of the difference in the thermal expansion coefficients between the ceramic catalyst layer and the metal substrate. A precipitation method based on a proprietary coating technique was applied to coat the Ru/Mg–Al oxide catalyst uniformly on the surface of the FeCralloy monoliths and foams to solve this problem [24,25]. The catalytic performances of the Ru/Mg–Al oxide-coated monoliths and foams in ammonia decomposition were investigated and compared. In addition, the foam catalysts were applied to a reactor in a 20 Nm^3/h high-purity H_2 production system, and their performance was evaluated for 100 h.

2. Experimental

2.1. Catalyst preparation

FeCralloy (Fe:72.8, Cr:22,Al:5, Y:0.1, Zr:0.1 wt%, Goodfellow Corp.) monolith and foam were used as metal-structured carriers. The diameter of the monolith was 22 mm, height was 20 mm, and cell density was 600–1000 cpi (cells/in^2). The foam with a thickness of 6.35 mm and a porosity of 20 and 40 ppi (pore per inch) was cut into a round shape (22 mm in diameter). The prepared monolithic catalysts and foam catalysts were designated as M_(cpi) and F_(ppi), respectively. The metal-structured carriers were rinsed with acetone and pre-calcined at 900 °C to form an Al_2O_3 layer on the metal substrate. Ru/Mg–Al oxide-coated metal-structured catalysts were prepared sequentially using a precipitation method based on the proprietary coating technique [24,25]. First, magnesium nitrate ($Mg(NO_3)_2 \cdot 6H_2O$, Aldrich) and aluminum nitrate ($Al(NO_3)_3 \cdot 9H_2O$, Aldrich) were employed as metal precursors to prepare an Mg–Al oxide support layer. The precursor solution was aged at 80 °C after adding urea as a precipitant. The coated Mg–Al oxide support layer was calcined at 900 °C in air. The Ru active metal was then coated using a ruthenium(III) nitrosyl nitrate solution ($Ru(NO)(NO_3)_x(OH)_y$, Aldrich) and ammonia solution as the metal precursor and precipitant, respectively.

2.2. Characterization

Inductively coupled plasma-mass spectrometry (ICP-MS 7700S, Agilent) was performed to measure the amount of Ru coating. The samples were pretreated in a mixed acid solution (70% HNO_3, 7 mL + 35% HCl, 3 mL) at 200 °C for 30 min using a microwave reaction. The Brunauer Emmett and Teller (BET) surface areas of the prepared metal-structured catalysts were measured on BELSORP-Max equipment (BEL Japan, Inc.). An in-house cell was used to measure the entire metal-structured catalyst sample. The sample was pretreated at 120 °C for 4 h under vacuum, followed by N_2 adsorption at −196 °C. Metal dispersion and Ru particle size were measured by chemisorption analysis (BEL-METAL-3, BEL Japan, Inc.). The metal-structured catalysts were cut to an appropriate size (approximately 0.3 g) and reduced at 600 °C for 3h in H_2 gas and then purged with He gas at 600 °C for 15 min. After cooling to 50 °C, a CO pulse was injected with 10 vol% CO/He mixed gas. The metal dispersion and particle size were estimated from the obtained CO adsorption, assuming an adsorption stoichiometry of CO/Ru = 1. The surface morphologies of the prepared metal-structured catalysts were analyzed using scanning electron microscopy (SEM, S-4700, Hitachi).

2.3. Catalytic test

A schematic of the experimental apparatus for ammonia decomposition is shown in Fig. 2. The test was carried out in a 1-inch Inconel tubular reactor (O.D. = 25.4 mm, I.D. = 22.1 nm) under reaction conditions of T = 550–700 °C, and gas hourly space velocity (GHSV) = 3,000–10,000 h^{-1} under atmospheric pressure. The thermocouple was placed at the bottom center of the catalyst bed. The catalysts were reduced at 600 °C for 3 h under 10%H_2/N_2 atmosphere before the reaction. The effluent consisted of H_2, N_2, and NH_3 and the residual NH_3 concentration (ppm) was measured using a gas analyzer (Airwell+7, KINSCO) via tunable diode laser absorption spectroscopy (TDLAS). HSC chemistry® 7.1 software was used to calculate the thermodynamic equilibrium value. NH_3 conversion (X_{NH3}) was calculated as follows:

$$X_{NH3}(\%) = \frac{F_{NH3,in} - F_{NH3,out}}{F_{NH3,in}} \times 100$$

where $F_{NH3,in}$ and $F_{NH3,out}$ are the mole flowrates (mol/min) of the inlet and outlet ammonia gases, respectively. For comparison, a commercial 0.5 wt% Ru/Al_2O_3 pellet catalyst (3 mm × 3 mm, AlfaAesar) was used as a reference.

3. Results and discussion

3.1. Catalytic characterization

The Ru contents, BET surface areas, Ru dispersions, and particle sizes of the prepared metal-structured catalysts are summarized in Table 1. Owing to the geometrical characteristics of the monolith and foam, the coated catalysts had different physical properties and active metal contents. The loaded Ru content was highest in the monolith catalyst (M_600) with a low cpi. This effect occurred because a higher cpi corresponded to narrower channel inlets, and did not favor the permeation of the precursor solution to owing to capillary action [22,26]. As the ppi of the foam catalyst increased, the cell window size and strut thickness decreased, increasing the porosity, geometric surface area (GSA), and S/V ratio [27]. The monolithic catalyst (M_800) and foam catalyst (F_40) with similar GSA and S/V ratios, had similar Ru contents (0.0014–0.0015 g). By contrast, the F_20 catalyst had a high Ru content of 0.0012 g, despite the halved GSA and S/V ratio values. The BET surface areas of the metal-structured catalysts were in the order M_600 > M_1000 > M_800 ≥ F_40 > F_20.

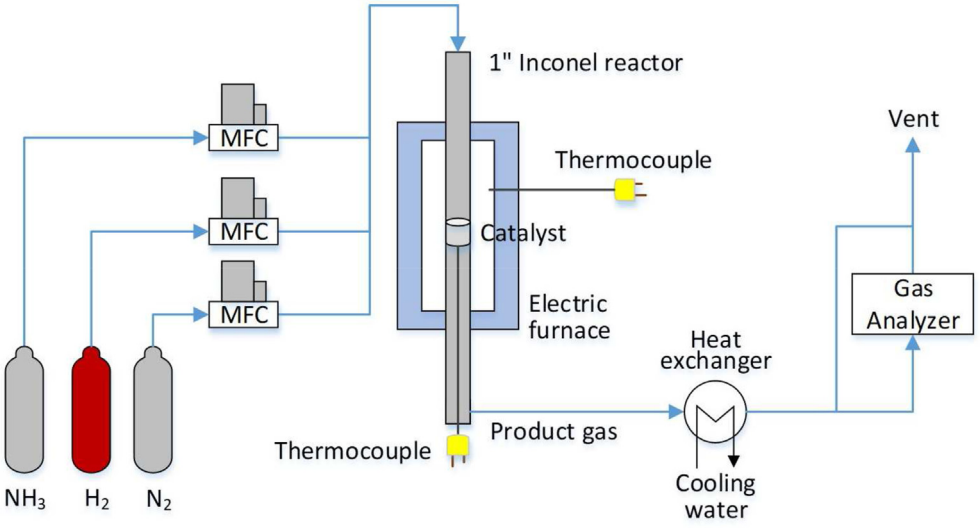

Fig. 2 – Schematic diagram of the experimental apparatus for NH_3 decomposition reaction system.

Table 1 – Characteristics of Ru-coated metal-structured catalysts and pellet catalyst.

Catalyst		GSA (m^2)	S/V (m^{-1})[a]	Ru content (wt%)[b]	Ru content (g)	BET surface area (m^2/g)[c]	Ru dispersion (%)[d]	Ru particle size (nm)[d]	Ru metal amount compared to Pellet ratio (%)
Monolith	M_600 (600 cpi)	3.89×10^{-2}	5,373	0.036	0.0024	143.3	19.3	6.92	15.2
	M_800 (800 cpi)	4.36×10^{-2}	5,939	0.020	0.0015	91.5	12.5	10.7	9.1
	M_1000 (1000 cpi)	5.03×10^{-2}	6,893	0.025	0.0023	100.8	15.7	8.53	14.1
Foam	F_20 (20 ppi)	2.05×10^{-2}	2,997	0.021	0.0012	62.1	16.0	8.37	7.2
	F_40 (40 ppi)	4.10×10^{-2}	5,994	0.030	0.0014	90.2	13.2	10.1	9.0
Pellet (0.5 wt% Ru/Al_2O_3)		6.27×10^{-3}	826	0.40	0.016	116.0	34.6	3.9	100

[a] Calculated using the catalyst packed volume: $7.60*10^{-3}$ L(monolith, pellet), $6.84*10^{-3}$ L(foam).
[b] Determined by ICP-MS.
[c] Estimated from N_2 adsorption at −196 °C.
[d] Estimated from CO-chemisorption at 50 °C.

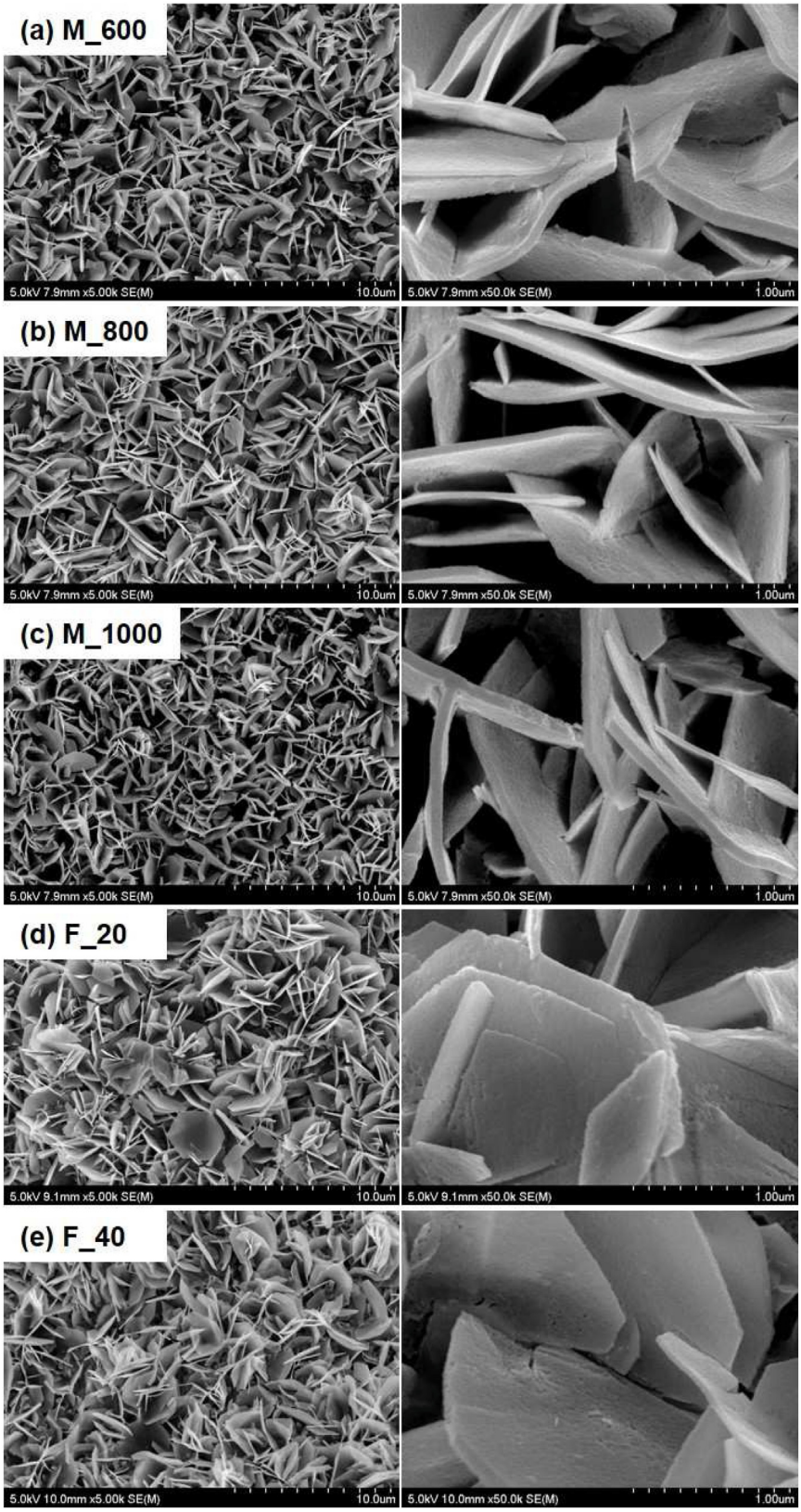

Fig. 3 – SEM images of Mg–Al oxide support layer coated on the FeCralloy metal substrate (a) M_600, (b) M_800, (c) M_1000, (d) F_20, (e) F_40.

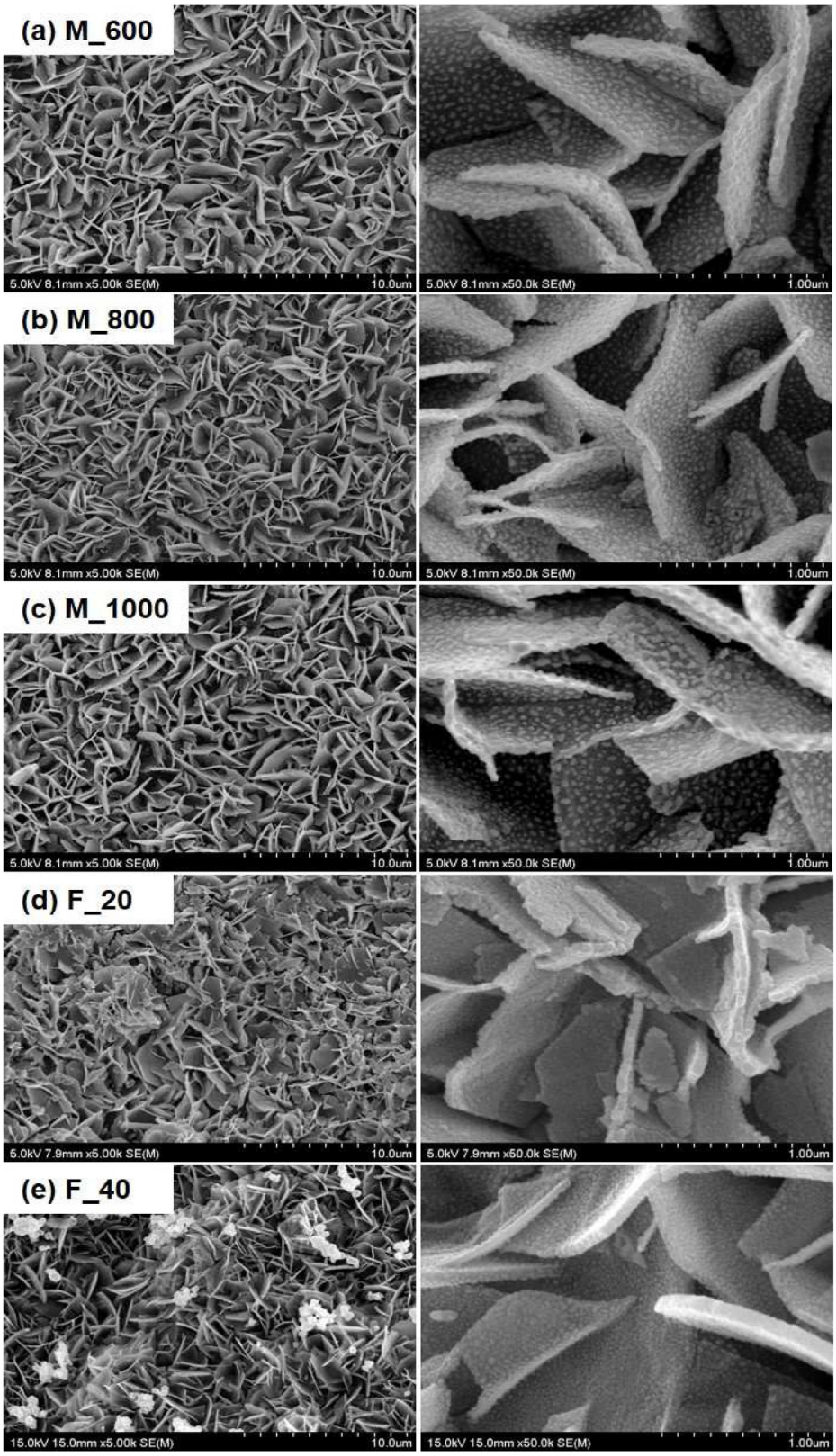

Fig. 4 – SEM images of Ru/Mg–Al oxide catalyst layer coated on the FeCralloy metal substrate (a) M_600, (b) M_800, (c) M_1000, (d) F_20, (e) F_40 (reduction: 600 °C, 3h).

By contrast, the Ru metal dispersion was in the following order M_600 > F_20 ≥ M_1000 > F_40 > M_800. Therefore, the geometry of the metallic structure had a marked effect on the Ru loading content, BET surface area, and Ru dispersion in the metal substrate. In particular, the amount of active metal in the structured catalyst was less than approximately 1/10 that in the pellet catalyst for the same reaction volume, i.e., a very small amount of Ru was uniformly coated as a thin layer on the metal substrate surface.

Fig. 3 shows the SEM images of the Mg–Al oxide support layer coated on the metal surface. A thin layer of plate-shaped Mg–Al oxide was uniformly formed on the monolith and foam surfaces. As mentioned previously, as the cell density of the monolith increased, the narrower and thinner monolith channels hindered the formation of a uniform coating. For the foam, the higher the ppi, the smaller and more complicated the pore size; this effect was unfavorable for developing uniform coatings on the internal part of the foam. However, it was confirmed that the precipitation-based coating method enabled uniform coating of the support layer on the metal surface, regardless of the geometric shape of the structure. In addition, the shapes and sizes of the Ru particles formed on the Mg–Al oxide support surface are shown in Fig. 4. Even after reducing the temperature to 600 °C, nanosized Ru particles (5–10 nm) were uniformly formed on the plate-shaped Mg–Al oxide support layer. In particular, the formation of spherical Ru particles was evident in the monolithic catalyst. Therefore, by applying the precipitation method, a small amount of active Ru metal could be uniformly loaded on the support layer surface.

3.2. *Catalytic test in ammonia decomposition*

The ammonia decomposition performance of the reference pellet catalyst (0.5 wt% Ru/Al_2O_3) was evaluated at various temperatures at GHSV = 3,000 h^{-1}. The unreacted ammonia concentration and ammonia conversion were compared to the thermodynamic equilibrium values calculated using the HSC (Fig. 5). The reaction results were markedly different from the equilibrium values at reaction temperatures lower than 600 °C. Therefore, the operating temperature had to be ≥ 600 °C for an actual ammonia decomposition reaction system. If the reaction conditions were set to ≤600 °C, excess catalyst was required, and the product gas composition could vary markedly, even with a small temperature change.

The Ru/Mg–Al oxide-coated metal-structured catalysts were tested for ammonia decomposition at 550–700 °C when the GHSV was 3,000 h^{-1}(Fig. 6). The concentration of unreacted ammonia decreased as the reaction temperature increased for all the structured catalysts. However, at low temperatures (≤600 °C), the performance of the Ru/Mg–Al oxide-coated catalyst was notably different from that of the pellet catalyst, indicating that the amount of catalyst was key to the reaction activity when the reaction rate was low. We hypothesized that M_800 and F_40, with similar catalyst loading amounts and BET surface areas, would show similar performances. However, M_800 demonstrated a significantly higher catalytic activity, suggesting that the catalytic performance also depends on the Ru loading condition on the metallic substrate of the monolith and foam (SEM images, in Fig. 4). As a result, the M_1000 and M_800 catalysts, with large BET surface areas, high catalyst loading, and uniform metal dispersions, showed the best performances. However, as the reaction temperature increased, most catalysts showed similar performance above 650 °C. At higher temperatures, the reaction rate increased. The differences in physical properties, such as the specific surface area, catalyst loading amount, and metal dispersion, had a negligible effect on the catalytic performance. It is worth noting that at a temperature ≥650 °C, the catalytic activities of metal-structured catalysts were equivalent to that of the pellet catalyst, although only 1/10 of the Ru active metal was used for the same reaction

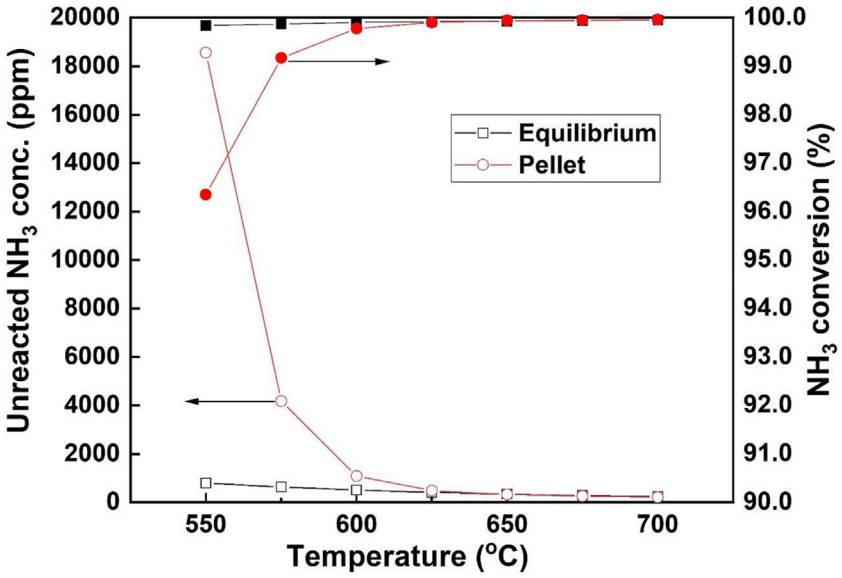

Fig. 5 – NH_3 conversion and residual NH_3 concentration using 0.5 wt% Ru/Al_2O_3 pellet catalyst in NH_3 decomposition reaction (reaction condition: T = 550–750 °C, GHSV = 3,000 h^{-1}).

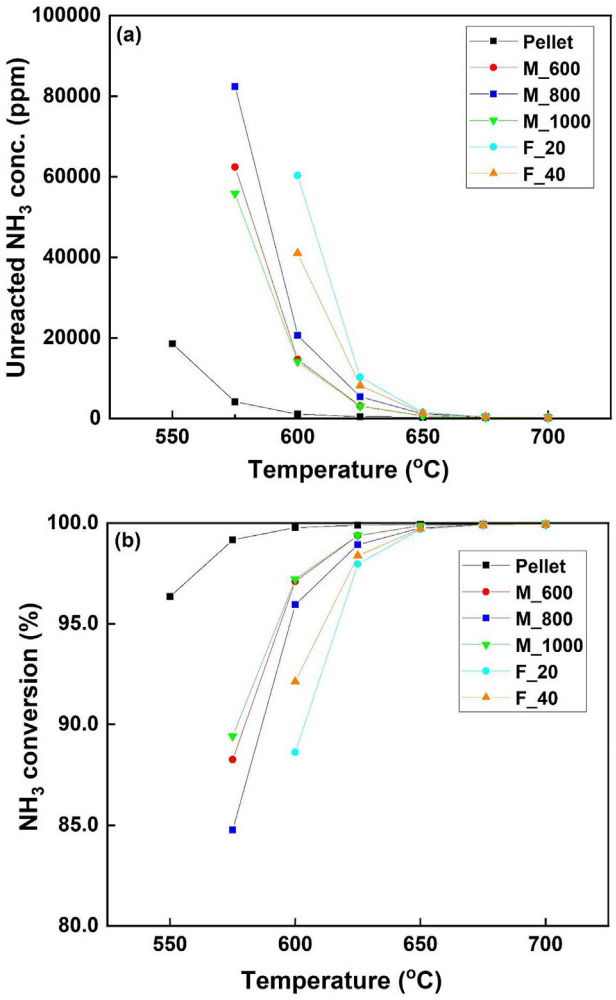

Fig. 6 – Comparison of (a) unreacted NH_3 concentration and (b) NH_3 conversion of metal structured catalysts for different reaction temperatures in NH_3 decomposition reaction (reaction condition: T = 550–750 °C, GHSV = 3,000 h^{-1}).

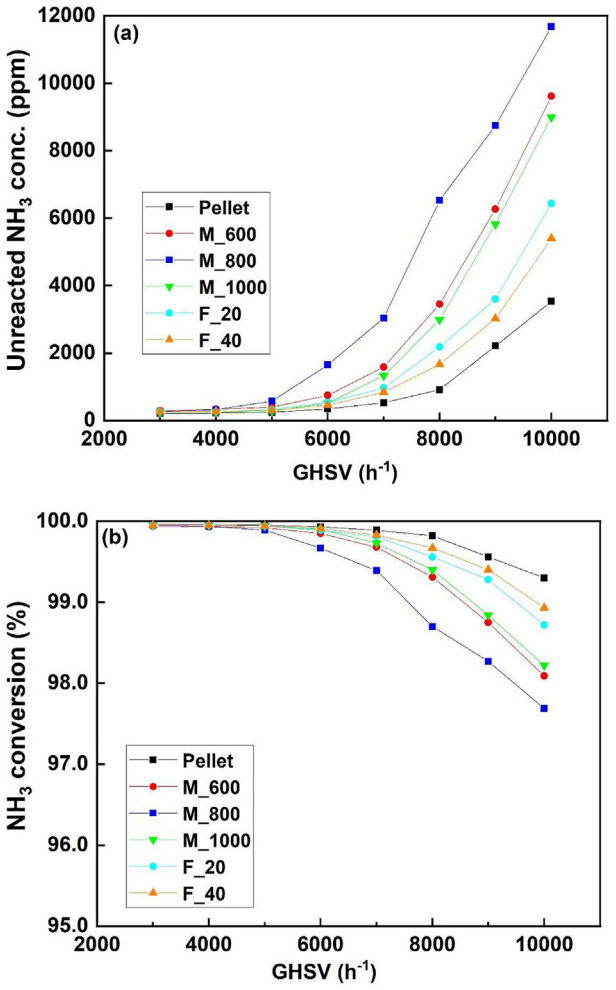

Fig. 7 – Comparison of (a) unreacted NH_3 concentration and (b) NH_3 conversion of metal structured catalysts for different GHSVs in NH_3 decomposition reaction (reaction condition: T = 700 °C, GHSV = 3,000–10,000 h^{-1}).

volume. Therefore, the uniformly coated Ru/Mg–Al oxide thin layer was expected to enable the design of a compact ammonia decomposition reactor by improving the heat transfer efficiency and reducing the amount of catalyst.

Fig. 7 shows the unreacted residual ammonia concentrations and ammonia conversions at different reaction gas flow rates at 700 °C. The unreacted residual ammonia concentration increased because a high GHSV caused a mass transfer limitation owing to the increased diffusion resistance [22]. In terms of catalytic activity, GHSV-dependent experiments showed different tendencies from those of the temperature-dependent experiments. In the temperature-dependent experiments, the M_1000 catalyst showed the best activity at low temperatures among the structured catalysts. By contrast, at high GHSV values, the F_40 catalyst showed the best activity. In addition, the F_20 catalyst with the lowest activity at low temperatures exhibited excellent performance in the GHSV-dependent experiments. When the GHSV increased, the reaction heat absorbed by the catalyst bed increased markedly. Therefore, heat transfer from external heat sources was extremely important. Generally, foams are suitable for low-pressure drop applications because of their high porosity and excellent mass transfer related to their complex pore structures and large geometric surface areas. In particular, foams can maintain a more uniform temperature distribution because of the improved thermal conductivity [28–30]. The wall temperature of the reaction tube in the foam catalysts was lower than those in the monolithic and pellet catalysts, confirming the excellent heat transfer in foams. However, foam catalysts were not suitable at low temperatures because of the low ammonia conversion under pressurized conditions. The foam catalyst was better than the monolithic catalyst at high GHSV (>6,000 h^{-1}) and high temperatures (>650 °C). Moreover, a high ppi value could be advantageous because of

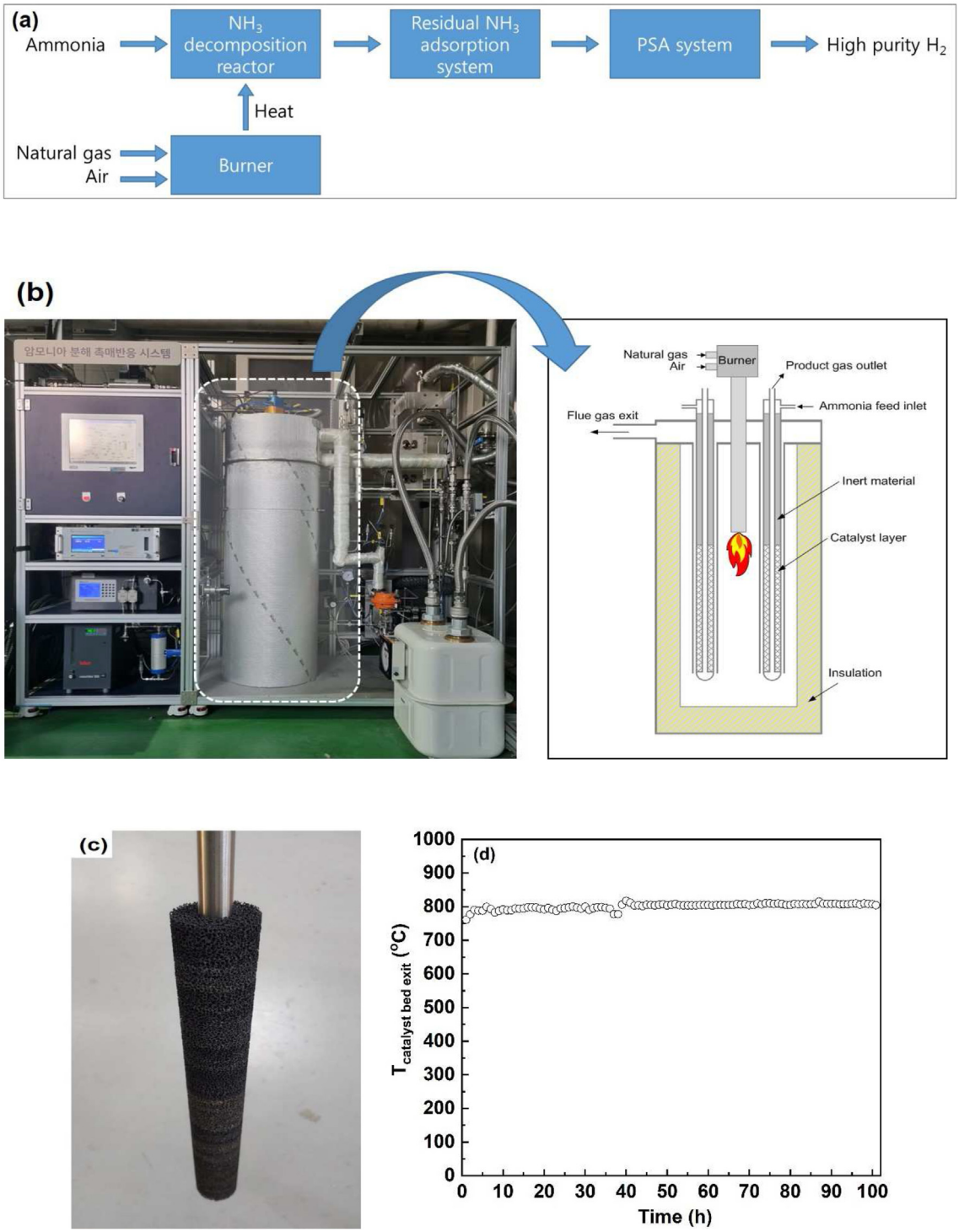

Fig. 8 – (a) Configuration of the NH_3-based high-purity hydrogen production system, (b) NH_3 decomposition reactor for 20 Nm^3/h-H_2 production, (c) Images of Ru/Mg–Al oxide coated foam catalysts, and (d) Average temperature of catalyst bed exit in stability test for 100 h (reaction condition: P = 8 bar, GHSV = 3,000 h^{-1}).

the increased surface area. However, differential pressures may be induced by the reactor shape and an appropriate ppi should be selected according to the reactant flow rate and reactor structure.

3.3. *20 Nm^3/h high-purity hydrogen production*

The ammonia-based high-purity hydrogen production system comprises a decomposition reactor, residual ammonia

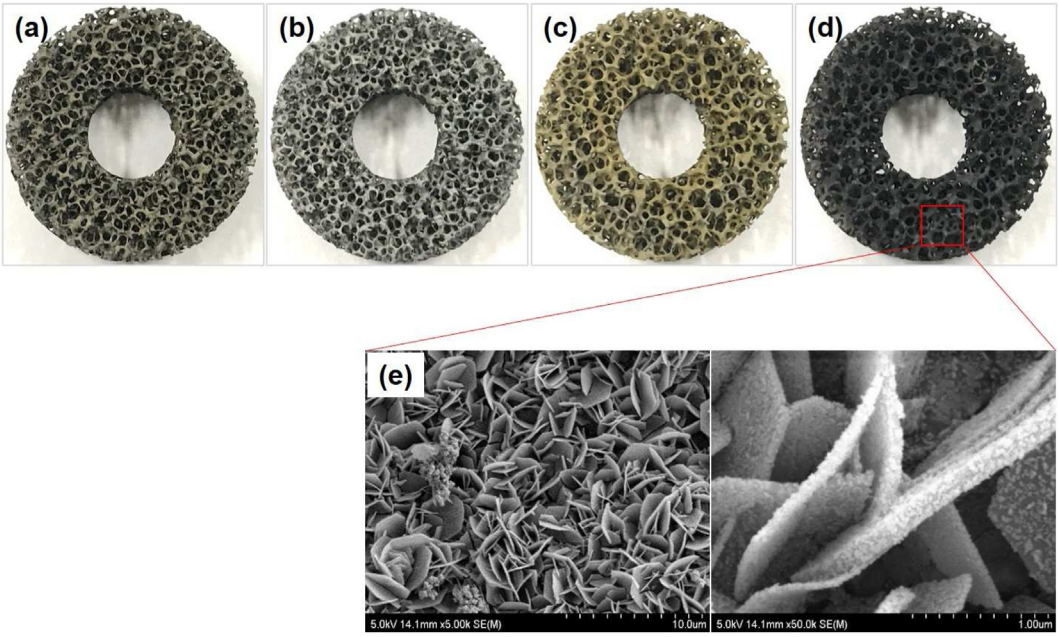

Fig. 9 – (a) FeCralloy bare foam, (b) Mg–Al oxide support coated foam, (c) Ru/Mg–Al oxide coated foam (before reduction), (d) Ru/Mg–Al oxide coated foam (after reduction at 600 °C, 3 h), and (e) SEM images of Ru/Mg–Al oxides coated foam catalysts applied for 20 Nm^3/h-H_2 production.

adsorption reactor, and PSA (Fig. 8(a)). The metal foam catalyst developed in this study was applied in the reactor a 20 Nm^3/h high-purity hydrogen production system. The ammonia decomposition reactor used natural gas as a heat source and eight heat exchange type tube reactors were arranged around a burner (Fig. 8(b)). The external diameter, internal diameter, and thickness of the donut-shaped foam catalyst were 43.2 mm, 15.9 mm, and 6.35 mm, respectively. Sixty catalysts in each reactor (480 metal foam catalysts in total) were used in the entire reactor (Fig. 8(c)). The experimental results of the ammonia decomposition reaction in the lab-scale 1″ reactor confirmed that the foam had better heat transfer properties than those of the monolith. In addition, 20 ppi foam was used in the ammonia decomposition reactor to minimize the differential pressure problem. Mg–Al oxide and Ru active metal were coated by sequential precipitation similar to the foam catalyst used in the 1″ reactor. By observing the foam catalyst after each stage of catalyst preparation, a clear color difference was observed in the Mg–Al oxide support layer coating and Ru catalyst coating before and after reduction (Fig. 9). The support layer and Ru active metal were uniformly coated on the entire surface of the foam. To confirm the stability of the metal foam catalyst coated with Ru/Mg–Al oxide, the catalyst was applied in an ammonia decomposition reactor and evaluated for 100 h (Fig. 8(d)). The operating pressure was maintained at 8 bar to ensure smooth operation of the PSA in the downstream of the reactor. The average temperature of the outlet of the metal foam catalyst layer was maintained at 800 °C, and the ammonia conversion was >99.0%. In addition, the ammonia conversion and the outlet temperature of the catalyst layer were well maintained for 100 h of cumulative operating time, indicating no deterioration in the performance of the metal foam catalyst. Moreover, high-purity hydrogen was produced through the ammonia decomposition reactor and the downstream process was applied to the PEMFC (proton-exchange membrane fuel cell) to stably generate electricity for 50 h (not detailed in this paper) [31–34].

4. Conclusions

Novel Ru/Mg–Al oxide-coated metal-structured catalysts have been applied in ammonia decomposition reaction to produce COx-free hydrogen. The Ru/Mg–Al oxide catalyst was uniformly coated as a thin layer on the surface of the FeCralloy monoliths and foams using the precipitation method. Ru particles with sizes of 5–10 nm were evenly dispersed on the surface of the wide-plate-shaped Mg–Al oxide support layer. In the ammonia decomposition reaction, the activity of the prepared metal-structured catalysts depended on the BET surface area, catalyst usage, and catalyst loading state. When the temperatures were ≤650 °C, the monolithic catalyst with a large specific surface area and evenly coated active metal layer exhibited excellent performance. By contrast, at temperatures ≥650 °C, the metal foam catalyst with excellent heat transfer properties displayed higher ammonia conversion at a high GHSV of 6,000 h^{-1}. In addition, at a temperature ≥650 °C, the metal-structured catalyst loaded with 1/10 of Ru exhibited ammonia decomposition activity equivalent to that of the pellet catalyst because of the improved heat transfer characteristics. The stability of the Ru/Mg–Al oxide-coated foam catalyst was verified in a 20 Nm^3/h high-purity hydrogen production system. Our study demonstrates that a compact and highly efficient ammonia decomposition reaction system can be developed on a large scale in the future by utilizing the Ru/Mg–Al oxide coated foam catalyst.

Declaration of competing interest

The authors declare that they have no known competing financial interests or personal relationships that could have appeared to influence the work reported in this paper.

Acknowledgement

This study was supported by the Ministry of Trade, Industry & Energy(MOTIE) and the Korea Institute of Energy Technology Evaluation and Planning(KETEP) of the Republic of Korea (No.20183010042020, No.20213030040550).

REFERENCES

[1] Cozzi L, Gül T. Net zero by 2050: a roadmap for the global energy sector. International Energy Agency (IEA); 2021. http://iea.li/nzeroadmap. [Accessed 4 January 2023].
[2] Guo J, Chen P. Catalyst: NH_3 as an energy carrier. Chem 2017;3(5):709–12. https://doi.org/10.1016/j.chempr.2017.10.004.
[3] Lamb KE, Dolan MD, Kennedy DF. Ammonia for hydrogen storage; A review of catalytic ammonia decomposition and hydrogen separation and purification. Int J Hydrogen Energy 2019;44(7):3580–93. https://doi.org/10.1016/j.ijhydene.2018.12.024.
[4] Lucentini I, Garcia X, Vendrell X, Llorca J. Review of the decomposition of ammonia to generate hydrogen. Ind Eng Chem Res 2021;60:18560–611. https://doi.org/10.1021/acs.iecr.1c00843.
[5] Lan R, Irvine JTS, Tao S. Ammonia and related chemicals as potential indirect hydrogen storage materials. Int J Hydrogen Energy 2012;37(2):1482–94. https://doi.org/10.1016/j.ijhydene.2011.10.004.
[6] Makhloufi C, Kezibri N. Large-scale decomposition of green ammonia for pure hydrogen production. Int J Hydrogen Energy 2021;46(70):34777–87. https://doi.org/10.1016/j.ijhydene.2021.07.188.
[7] Morlanés N, Katikaneni SP, Paglieri SN, Harale A, Solami B, Sarathy SM, et al. A technological roadmap to the ammonia energy economy: current state and missing technologies. Chem Eng J 2021;408:127310. https://doi.org/10.1016/j.cej.2020.127310.
[8] Lin L, Tian Y, Su W, Luo Y, Chen C, Jiang L. Techno-economic analysis and comprehensive optimization of an on-site hydrogen refuelling station system using ammonia: hybrid hydrogen purification with both high H_2 purity and high recovery. Sustain Energy Fuels 2020;4(6):3006–17. https://doi.org/10.1039/C9SE01111K.
[9] Beurey C, Gozlan B, Carré M, Bacquart T, Morris A, Moore N, et al. Review and survey of methods for analysis of impurities in hydrogen for fuel cell vehicles according to ISO 14687:2019. Front Energy Res 2021;8(20):615149. https://doi.org/10.3389/fenrg.2020.615149.
[10] Bacquart T, Moore N, Storms W, Chramosta N, Morris A, Murugan A, et al. Hydrogen fuel quality for transport – first sampling and analysis comparison in Europe on hydrogen refueling station (70 MPa) according to ISO 14687 and EN 17124. Fuel Commun 2021;6:100008. https://doi.org/10.1016/j.jfueco.2021.10 0 0 08.
[11] Ratnasamy C, Wangner JP. Water gas shift catalysis. Catal Rev 2009;51(3):325–440. https://doi.org/10.1080/01614940903048661.
[12] Chiuta S, Everson RC, Neomagus HWJP, van der Gryp P, Bessarabov DG. Reactor technology options for distributed hydrogen generation via ammonia decomposition: a review. Int J Hydrogen Energy 2013;38(35):14968–91. https://doi.org/10.1016/j.ijhydene.2013.09.067.
[13] Le TA, Do QC, Kim Y, Kim T-W, Chae H-J. A review on the recent developments of ruthenium and nickel catalysts for COx-free H_2 generation by ammonia decomposition. Kor J Chem Eng 2021;38(6):1087–103. https://doi.org/10.1007/s11814-021-0767-7.
[14] Li X-K, Ji W-J, Zhao J, Wang S-J, Au C-T. Ammonia decomposition over Ru and Ni catalysts supported on fumed SiO_2, MCM-41, and SBA-15. J Catal 2005;236(2):181–9. https://doi.org/10.1016/j.jcat.2005.09.030.
[15] Li D, Li R, Lu M, Lin X, Zhan Y, Jiang L. Carbon dioxide reforming of methane over Ru catalysts supported on Mg-Al oxides: a highly dispersed and stable Ru/Mg(Al)O catalyst. Appl Catal B Environ 2017;200:566–77. https://doi.org/10.1016/j.apcatb.2016.07.050.
[16] Dahdah E, Aouad S, Gennequin C, Estephane J, Nsouli B, Aboukaïs A, et al. Glycerol steam reforming over Ru-Mg-Al hydrotalcite-derived mixed oxides: role of the preparation method in catalytic activity. Int J Hydrogen Energy 2018;43(43):19864–72. https://doi.org/10.1016/j.ijhydene.2018.09.042.
[17] Kehres J, Jakobse G, Andreasen JW, Wagner JB, Liu H, Molenbroek A, et al. Dynamical properties of a $Ru/MgAl_2O_4$ catalyst during reduction and dry methane reforming. J Phys Chem C 2012;116(40):21407–15. https://doi.org/10.1021/jp3069656.
[18] Li LD, Yu JJ, Hao ZP, Xu ZP. Novel Ru-Mg-Al-O catalyst derived from hydrotalcite-like compound for NO storage/decompsotion/reduction. J Phys Chem C 2007;11(28):10552–9. https://doi.org/10.1021/jp0678352.
[19] Jacobsen CJH, Dahl S, Hansen PL, Törnqvist E, Jensen L, Topsøe H, et al. Structure sensitivity of supported ruthenium catalysts for ammonia synthesis. J Mol Catal 2000;163(1/2):19–26. https://doi.org/10.1016/S1381-1169(00)00396-4.
[20] Szmigiel D, Raróg-Pilecka W, Miśkiewicz E, Kaszkur Z, Kowalczyk Z. Ammonia decomposition over the ruthenium catalysts deposited on magnesium-aluminum spinel. Appl Catal, A 2004;264(1):59–63. https://doi.org/10.1016/j.apcata.2003.12.038.
[21] Su Q, Gu LL, Zhong AH, Yao Y, Ji WJ, Ding WP, Au CT. Layered double hydroxide derived Mg_2Al-LDO supported and K-modified Ru catalyst for hydrogen production via ammonia decomposition. Catal Lett 2018;148:894–903. https://doi.org/10.1007/s10562-017-2195-1.
[22] Koo KY, Eom HJ, Jung UH, Yoon WL. Ni nanosheet-coated monolith catalyst with high performance for hydrogen production via natural gas steam reforming. Appl Catal, A 2016;525:103–9. https://doi.org/10.1016/j.apcata.2016.07.016.
[23] Sirijaruphan A, Goodwin Jr JG, Rice RW, Wei D, Butcher KR, Roberts GW, et al. Metal foam supported Pt catalysts for the selective oxidation of CO in hydrogen. Appl Catal, A 2005;281:1–9. https://doi.org/10.1016/j.apcata.2004.10.019.
[24] Koo KY, Eom HJ, Kwon SC, Jung UH, Yoon WL. Ru-coated metal monolith catalyst prepared by novel coating method for hydrogen production via natural gas steam reforming. Catal Today 2017;293–294:129–35. https://doi.org/10.1016/j.cattod.2016.11.016.
[25] Lee TH, Jung U, Im HB, Kim KD, Kim J, Kim Y, et al. Comparative evaluation of Ru-coated fecralloy and SiC monolithic catalysts in catalytic partial oxidation of natural

gas for hydrogen production. J Ind Eng Chem 2022;110:178–87. https://doi.org/10.1016/j.jiec.2022.02.050.
[26] Meille V. Review on methods to deposit catalysts on structured surfaces. Appl Catal, A 2006;315:1–17. https://doi.org/10.1016/j.apcata.2006.08.031.
[27] Zhang H, Suszynski WJ, Agrawal KV, Tsapatsis M, Al Hashimi SA, Francis LF. Coating of open cell foams. Ind Eng Chem Res 2012;51:9250–9. https://doi.org/10.1021/ie300266p.
[28] Razza S, Heidig T, Bianchi E, Groppi G, Schwieger W, Tronconi E, et al. Heat transfer performance of structured catalytic reactors packed with metal foam supports: influence of wall coupling. Catal Today 2016;273:187–95. https://doi.org/10.1016/j.cattod.2016.02.058.
[29] Xia X-L, Chen X, Sun C, Li Z, Liu B. Experiment on the convective heat transfer from airflow to skeleton in open-cell porous foams. Int J Heat Mass Tran 2017;106:83–90. https://doi.org/10.1016/j.ijheatmasstransfer.2016.10.053.
[30] Settar A, Nebbali R, Madani B, Abboudi S. Numerical investigation on the wall-coated steam methane reformer improvement: effects of catalyst layer patterns and metal foam insertion. Int J Hydrogen Energy 2015;40(15):8966–79. https://doi.org/10.1016/j.ijhydene.2015.04.100.
[31] Koo KY, Im HB, Song D, Jung U. Status of COx-free hydrogen production technology development using ammonia. J Energy & Climate change 2019;14:34–42.
[32] Yoon HC. Production and utilization of green ammonia: KIER's current status and future plans. Ammonia Energy Conference. Australia 2021:25–7. August 2021.
[33] Jung U, Im HB, Koo KY. Development of highly efficient ammonia cracker for green hydrogen production. Gwangju: Korea Society of energy & climate change 2021; 2021.
[34] Korea Institute of Energy Research (KIER) develops core technology to extract hydrogen from ammonia. South Korea: Monthly Hydrogen Economy Corporation; 2021. https://www.h2news.kr/news/article.html?no=9178. [Accessed 7 January 2023].